Progress In Electromagnetics Research, PIER 93, 221–236, 2009

COMPOSITE COMPACT TRIPLE-BAND MICROSTRIP ANTENNAS

M. A. S. Alkanhal

Department of Electrical Engineering
King Saud University
P. O. Box: 800, Riyadh 11421, Saudi Arabia

Abstract—Two new triple band small size composite-resonator microstrip antenna configurations for wireless communications are presented in this paper. The proposed antennas, each is built of three resonant elements. Two types of compact short-circuited resonators are used; stepped impedance and quarter-wave resonators. The design procedure based on composing the antenna resonators is straightforward and can be applied to design any triple band antenna at three pre-specified bands using simple relations and design curves. The resonator integration has been performed to maintain single feed, reduce the overall antenna size, and preserve the quality-performance at each band. The two designed antennas are simulated, optimized, and realized on RT/Duroid substrate to verify the concept. Simulation and experimental results are in good agreement and demonstrate the performance of both triple band compact antennas.

1. INTRODUCTION

Antennas for portable cellular phones are required to be small in size and light in weight. Microstrip antennas (MSAs) have the attractive features of low profile, small size, low cost, and conformability to mounting hosts which makes them excellent candidates for satisfying this design consideration. Recently, many novel planar antenna designs to satisfy the requirements of mobile cellular communication systems have been developed. These systems include global system for mobile communication (GSM; 890–960 MHz), digital communication system (DCS; 1710–1880 MHz), personal communication system (PCS; 1850–1990 MHz), and the universal mobile telecommunication system

Corresponding author: M. A. S. Alkanhal (majeed@ksu.edu.sa).

(UMTS; 1920–2170 MHz). Planar antennas are also very attractive for applications in communication devices for global poisoning system (GPS; 1575.24 MHz), and wireless local area network (WLAN) systems in the 2.4 GHz (2400–2484 MHz) and 5.2 GHz (5150–5350 MHz) bands.

In many applications, operation in two or more discrete bands is desired. The trend in the development of wireless personal communication systems has been in the pursuit of a single system that can accommodate the needs of all users. In such cases, a patch antenna capable of operating in multi-band is highly desirable. The design of compact multiple band microstrip antennas for wireless applications has recently received much attention [1–17]. Several PIFA configurations have been suggested for GSM/DCS/WLAN, 900/1800/2450 MHz bands in recent publications. A PIFA that consists of three separate short-circuited patches with a triple feed integrated in a compact structure is presented in [12]. Another PIFA structure has been designed in order to reduce the number of feeders used in the above case, and hence simplifies the structure and reduces the cost [13]. A meander patch PIFA structure has been suggested to use only single feed instead of triple or dual feeds as in the above two cases. Moreover, the structure uses two shorting pins. Branch line strip PIFA has also been proposed for triple band operation [14]. In that multilayer structure, two short-circuited branch strips are used. Single feed is located in an appropriate location to provide good matching at the three bands. These antenna strips are printed on FR4 substrate of thickness 3.2 mm and relative permittivity 4.4. Between the FR4 substrate and the ground plane there is another layer of air substrate of thickness 2.3 mm. Plastic posts are used to support the FR4 substrate on the ground plate. More recently, a triple-band omni-directional antenna which comprises three pairs of dipoles placed back to back and printed on a dielectric substrate has been suggested for WLAN applications [17]. Most of the above described contributions and other published work are based, generally, on experience intuition and trial and error schemes. Antenna design based on such methods will make the offered multiband-matched antenna configurations intricate to be directly-reproduced.

In this paper, a simple procedure to design triple band composite antenna-geometries based on multiple resonator integration is described. Two compact simple composite microstrip antenna configurations that operate at three different pre-selected frequencies are designed utilizing this outlined method. Each configuration consists of three resonant elements. Each resonator-element can be directly-designed separately at a specific frequency and, then, integrated in such a way that the structure maintains compact shape

and good matching at the three distinct bands using a single feed-probe and single shorting-probe only. The first antenna structure is based on integration of reduced-size short-circuited stepped impedance resonators. The lumped element model driven from the transmission line theory can be used to predict the resonance frequencies of the stepped impedance elements as described in the next section. The second triple-band antenna configuration is a modified E-shaped compact configuration that uses simple uniform short-circuited quarter-wave resonator elements. The first antenna configuration is investigated in the next section and the second is presented in Section 3.

2. TRIPLE BAND ANTENNAS COMPOSED OF SHORT CIRCUITED STEPPED IMPEDANCE RESONATORS

A basic microstrip patch antenna is a resonant-type radiator so one of its dimensions must be approximately $\lambda_g/2$, where λ_g is the guided wavelength. The properties of the substrate, namely, its dielectric constant (ε_r) and its height play a fundamental role in the performance of the printed antenna. The size of an antenna based even on a quarter wavelength line is physically too large to be used at 900 MHz, especially when designed on low permittivity substrates to enhance bandwidth and efficiency. For this reason, usually, a shaped short circuit resonator such as short-circuited H-structure [18] or T-shape [19] is used for single frequency operation. As shown in Fig. 1, the proposed triple-band antenna consists of three resonant elements. Two types of resonators

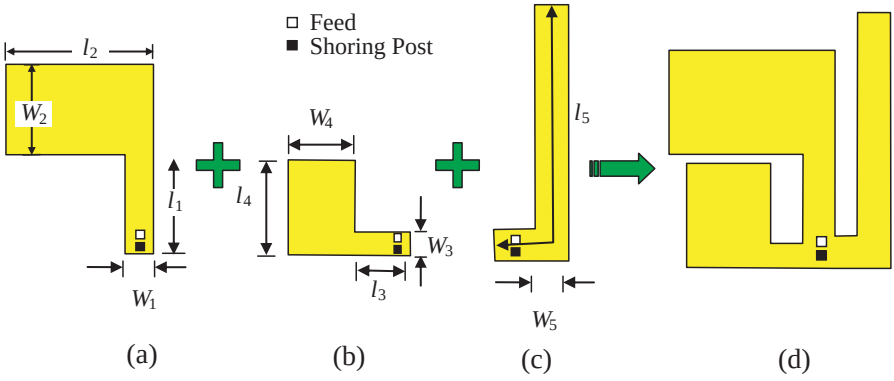

Figure 1. Composing the triple-band antenna. (a) L-shaped antenna that operates at the lower frequency. (b) L-shaped antenna that operates at the higher frequency. (c) Short circuited bent resonator. (d) Geometry of the proposed composite triple band antenna.

are used in this structure. The first one is a short-circuited stepped impedance structure, and the second one is simply a bent uniform short circuited line. The stepped impedance resonator in Fig. 1(a), designed to operate at the lower frequency, consists of two sections with physical lengths l_1 and l_2 and widths W_1 and W_2. Moreover, the stepped impedance resonator in Fig. 1(b), designed to operate at the higher frequency, consists of two sections with physical lengths l_3 and l_4 and widths W_3 and W_4. The quarter wave resonator shown in Fig. 1(c) of 90° effective electrical length will be designed to operate at the middle frequency. Its physical length and width are denoted by l_5 and W_5, respectively. The lumped element model driven from the transmission line theory can be used to predict the resonance frequencies of the stepped impedance elements.

2.1. Lumped Circuit Equivalence of the Antenna Elements

A microstrip antenna resonator can be modeled as a resonant circuit. The simplest microstrip resonators are a half wavelength line opened at both ends and a quarter wavelength line opened at one end and short-circuited at the other end. The effective electrical length of any short circuited resonator is 90 degrees. The analysis and design of the stepped impedances resonators can be achieved using transmission line theory and their equivalent lumped element circuits. Referring to the stepped impedance resonator geometry shown in Fig. 1(a), let the characteristic impedance of the narrower microstrip line to be Z_1 and its electrical length to be θ_1. Similarly, let the characteristic impedance of the wider microstrip line to be Z_2 and its electrical length to be θ_2. The discontinuity effect is included in calculating characteristic

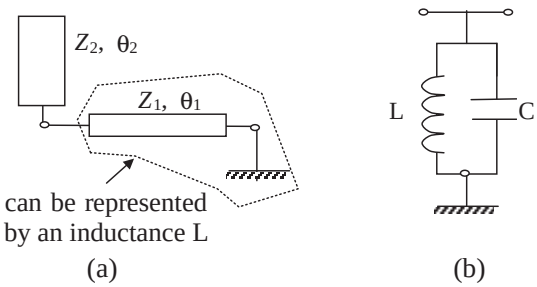

Figure 2. The stepped impedance resonator-antenna model. (a) Transmission line equivalence of antenna elements in Figs. 1(a) and 1(b). (b) Lumped element equivalence of the resonators in Figs. 1(a) and 1(b).

impedances of the microstrip lines. The transmission line equivalence of the short-circuited stepped impedance resonator element is shown in Fig. 2. The lumped elements are calculated for each antenna using transmission line theory.

The short-circuited line is equivalent to a lumped inductance as

$$\omega L = Z_1 \tan\theta_1 \tag{1}$$

where $\theta_1 = \omega l_1/v_{ph1}$, v_{ph1} and Z_1 are the phase velocity and characteristic impedance of the narrower lines. The capacitance of the parallel open lines is related to their physical dimensions by

$$\omega C = Y_2 \tan\theta_2 \tag{2}$$

where $\theta_2 = \omega l_2/v_{ph2}$, v_{ph2} and Y_2 are the phase velocity and characteristic admittance $(1/Z_2)$ of the wider lines. Combining (1) and (2) at the resonant frequency $\omega = \omega_0 = 1/\sqrt{LC}$, we get

$$\tan\theta_1 \tan\theta_2 = K \tag{3}$$

at resonance, where K is the ratio of the line impedances; $K = Z_2/Z_1$. Equation (3) is utilized to plot θ_2 against θ_1 for different values of K in Fig. 3. It is observed that, for a certain value of θ_1, θ_2 decreases as K decreases resulting in a reduction of the total antenna size. The total electrical length of the antenna is given by $\theta_t = \theta_1 + \theta_2$.

For $K = 1$ (uniform resonator), the total electrical length is 90° and the total length decreases as K decreases. Fig. 3 is a helpful tool for basic designs of each antenna element through judicial selection

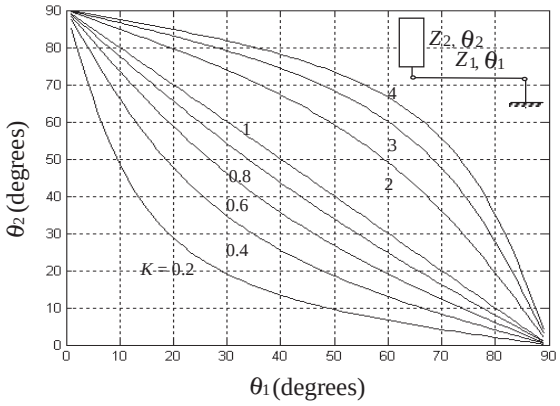

Figure 3. θ_1 versus θ_2 for different values of K.

of the K factor, and hence the selection of electrical lengths of the antenna arms [19].

The antenna physical dimensions l_1, l_2, W_1, and W_2, of the antenna element at the lower band and l_3, l_4, W_3, and W_4 for the element at the higher frequency band can be calculated for specific frequencies of operation as will be described in the next section.

2.2. Composing the Stepped Impedance Triple-Band Antenna

The concept of composing components of this triple band antenna is illustrated in Fig. 1. First, two L-shaped stepped impedance components are designed to operate at 900/1800 MHz GSM/DCS1800 bands [20]. Thereafter, a third resonant element is added for operation at the third band of 1500 MHz (GPS band). RT/Duroid dielectric substrate with $\varepsilon_r = 2.2$ and thickness, $h = 1.57$ mm is used to demonstrate the design concept. The width of the narrow line is chosen to be 4 mm for both elements to avoid degradation of the antenna efficiency and the width of the wider line is selected for a suitable value of the impedance ratio K to achieve antenna size reduction and concurrently to maintain the validity of transmission line analysis of the resonators. We choose $W_2 = W_4 = 10$ mm to provide a suitable radiation aperture at the 900/1800 MHz bands. The characteristic impedances corresponding to these dimensions are $Z_1 = Z_3 = 56.5\,\Omega$ and $Z_2 = Z_4 = 29.5\,\Omega$ giving a K value of 0.52. For the inverted L-shaped element, in Fig. 1(a), that operates at the lower band, either Equation (3) or Fig. 3 can be used for direct element design. This indicates that for $\theta_1 = 32^\circ$, θ_2 is 40° for that element. The physical size of this structure, calculated at 900 MHz considering discontinuity effects, are $l_1 = 18$ mm and $l_2 = 28$ mm.

To demonstrate the antenna performance, simulation results of the input return loss (S_{11}), using a full electromagnetic (EM) simulator, are given in Fig. 4. The simulated resonance frequency at the lower band is 907 MHz. For good matching, a probe feed of radius 0.5 mm is located 1.8 mm from the shorting post of 0.5 mm radius. Similar steps are used to design the L-shaped antenna element to operate at 1.8 GHz. The same line widths are used and the electrical lengths are obtained from either Fig. 3 or Equation (3). The physical dimensions are $l_3 = 6$ mm and $l_4 = 17.5$ mm. The simulation results for this L-shaped element are shown in Fig. 5 where the simulated resonance frequency is at 1.808 GHz. The same feeder and the shorting post are used and made common for the two elements. The bandwidths determined from 1 : 2.5 VSWR, are about 5 and 18 MHz in the 900 and 1800 MHz bands, respectively. The two resonant elements are then integrated as

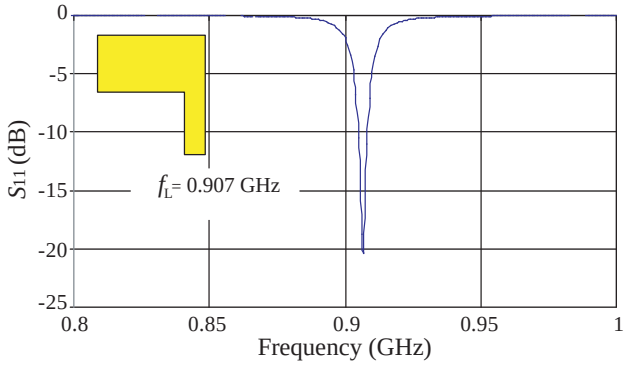

Figure 4. Computed S_{11} of the stepped resonator element at the lower band (900 MHz).

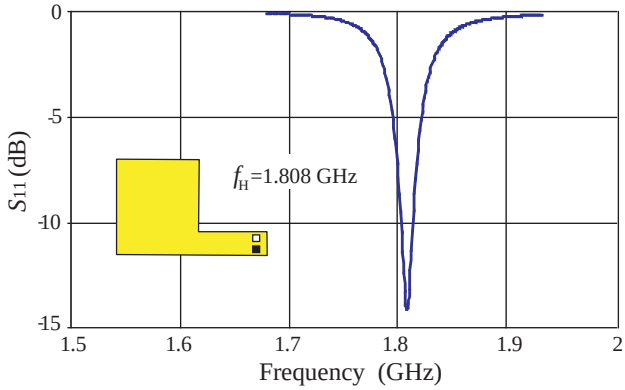

Figure 5. Computed S_{11} of the stepped resonator element at the higher band (1800 MHz).

shown in the inset of Fig. 6. It is noted that locating the shorting post at the edge of both elements, almost, eliminates the mutual loading of one element on the other. Matching is also observed for the composite structure since matching depends mostly on the relative distance between the feeder and the short circuit. The simulation result of the composite antenna structure is shown in Fig. 6. The lower and higher resonances occurs at $f_L = 907$ MHz and $f_H = 1800$ MHz, respectively. Slight changes in resonance frequencies are observed after integration. A further third resonator-element is essential for 1500 MHz operation. A simple short-circuited quarter wave resonator is added as shown in Fig. 7. This element is integrated in such a manner that

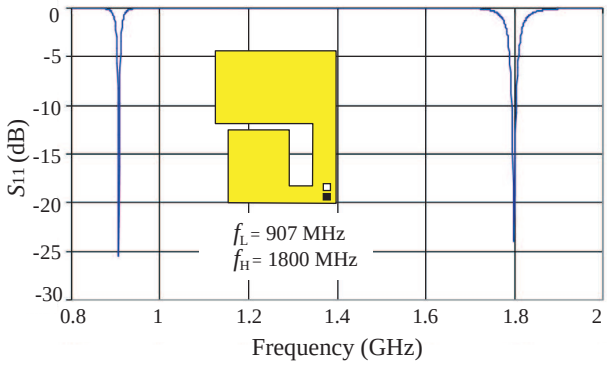

Figure 6. Computed S_{11} of the two-resonator dual band antenna.

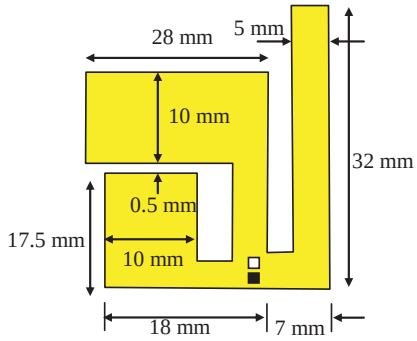

Figure 7. Top patch of the stepped impedance triple band antenna designed on RT/Duroid dielectric substrate of $\varepsilon_r = 2.2$, and thickness 1.57 mm.

the existing shorting post is utilized and positioned in the proper location in order to minimize the loading effect on the main dual band antenna. The simulated results are shown in Fig. 8. A little shift in resonance frequencies with respect to the dual band antenna of Fig. 6 is observed. The lower resonance frequency only shifted from 907 to 914 MHz. However the higher resonance shifted from 1800 to 1734 MHz. The frequency shift can be easily readjusted by simple increase or decrease in the lengths of the corresponding arms. For example, the higher frequency is readjusted to 1803 MHz by decreasing l_4 from 17.5 mm to 16.5 mm. The lower frequency resonance is moved to 905 MHz by increasing l_2 from 28 to 28.5 mm. Further adjustment

of the third resonator-element length is required to optimize the triple-band composite antenna performance.

3. TRIPLE BAND COMPACT MODIFIED E-SHAPED ANTENNAS

The second triple band antenna proposed in this paper is consisted of three short circuited resonant elements integrated using the same approach described in the previous section. In this composite antenna, the three resonant elements are simple bent uniform lines that are integrated as shown in Fig. 9. The resulted composite configuration

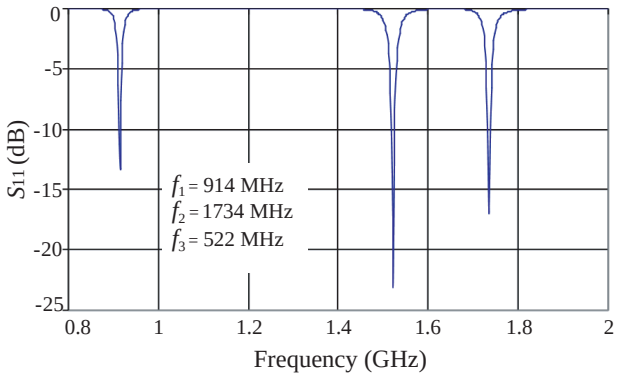

Figure 8. Computed S_{11} of the stepped impedance triple band antenna.

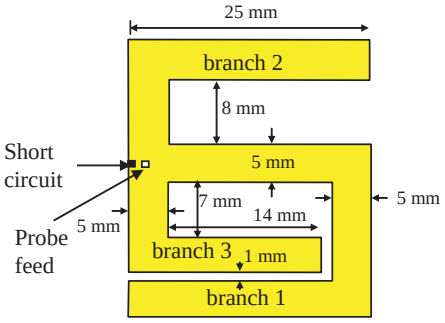

Figure 9. Top patch of the modified E-shaped triple band antenna designed on RT/Duroid dielectric substrate of $\varepsilon_r = 2.2$, and thickness 1.57 mm.

is a modified E-shaped structure. The bandwidth of that antenna could be improved at the cost of its size-increase. A single feed, only, is used for the achieved triple band operation. The geometry of this antenna is printed on RT/Duroid dielectric substrate with $\varepsilon_r = 2.2$ and thickness 1.57 mm. The longer resonator (branch 1) controls the excitation of the resonant frequency at about 900 MHz, the shorter resonator (branch 3) controls the resonant frequency at about 1800 MHz, and the medium length resonator (branch 2) controls the resonance at about 1500 MHz. The three branches are connected at the T-junction making the feed and short circuit posts common for all branches. The effect of the T-junction is modeled and simulated in order to define the reference planes and then define the length of each branch. The bends as well as the open ends have also been modeled and their effect is compensated in the final configuration. The simulated results are shown in Fig. 10. The simulated resonance frequencies are 892 MHz, 1506 MHz, and 1871 MHz. The impedance bandwidths of the three frequency bands, determined from 1 : 2.5 VSWR or about 7.3 dB return loss, are about 5 MHz (about 0.56%), 12 MHz, (about 0.8%), and 11 MHz (about 0.59%) at the lower, medium, and higher bands, respectively.

4. BANDWIDTH ENHANCEMENT OF THE COMPOSITE ANTENNA STRUCTURES

One of the most effective techniques for improving the bandwidth of compact antennas is chip-resistor loading but at the expense of the

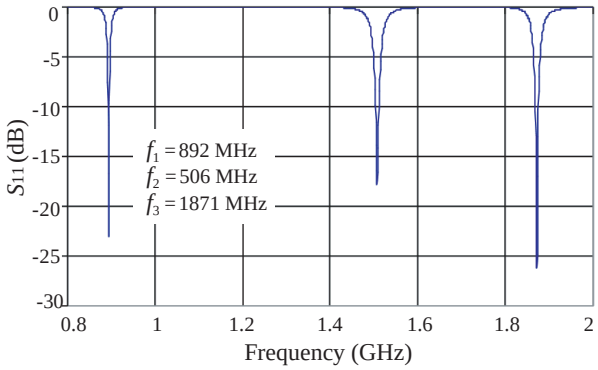

Figure 10. Computed S_{11} of the proposed modified E-shaped triple band antenna.

antenna efficiency and gain [21–23]. Designs of a chip-resistor loaded single-band MSAs fed using a probe or inset microstrip lines have been reported [21, 22]. The bandwidth of the triple band antenna configuration of Fig. 7 have been enhanced by replacing the short-circuit post by a resistive post. However, feeder adjustment for simultaneously matching the three bands must be carried out carefully. Also, the antenna dimensions have been slightly optimized in order to preserve the same resonance frequencies. The final structure has been designed with a $2\,\Omega$ resistive post with the feeder moved 5 mm away from the resistive post. The bandwidths at the resonance frequencies, determined from 1 : 2.5 VSWR or about 7.3 dB return loss, are of about 40 MHz (about 4.4%), 14 MHz (about 0.9%), and 80 MHz (about 4.4%), respectively.

For the modified E-shaped antenna structure shown in Fig. 9, a $1.5\,\Omega$ resistance is inserted instead of the short circuit. The feeder is appropriately located at 7 mm distance from the resistive post in order to maintain matching at the three bands. The three frequency bands, determined from 1 : 2.5 VSWR or about 7.3 dB return loss, have impedance bandwidths of about 50 MHz (about 5.6%), 20 MHz (about 1.3%), and 46 MHz (about 2.4%), respectively.

With the above mentioned bandwidth remedy, it is estimated that the antenna gain will be approximately 1.5 dB lower than that of the short circuited patch; that is the bandwidth enhancement is at some expense of antenna gain [22].

5. RADIATION CHARACTERISTICS

To examine the radiation of the composite triple band antenna structures, the radiation pattern and coexisting current distribution of the triple band modified E-shaped antenna of Fig. 7 are depicted in Fig. 11 to Fig. 13. The studied far field radiation patterns E_θ at $\phi = 0°$ and 90° and current distribution at the three 900 MHz, 1500 MHz, and 1800 MHz bands show that: (1) the current in each branch dominates only at the resonance frequency of the branch element, (2) the three radiations patterns at the three bands are similar to each other and are even patterns, with less than 9 dB level variations, which is appropriate for mobile handset applications. The radiation results of the stepped impedance triple band antenna structure are very similar to that shown above. Typical antenna structures in handheld mobile sets are commonly realized on air substrates with considerable heights. Thick low permittivity substrates physically enhance the efficiency and bandwidth of printed antennas.

6. EXPERIMENTAL VALIDATION

In order to verify the design approach presented in this paper, the modified E-shaped antenna shown in Fig. 9 is implemented on the same

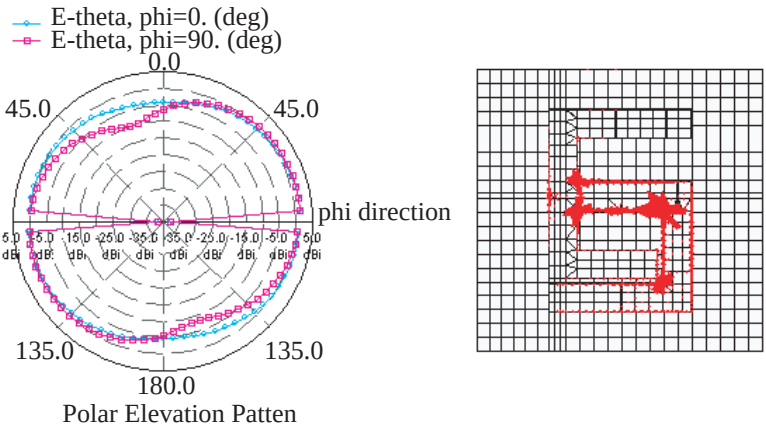

Figure 11. Radiation pattern and current distribution at the first resonance (900 MHz band). (a) Radiation pattern, (b) Current distribution.

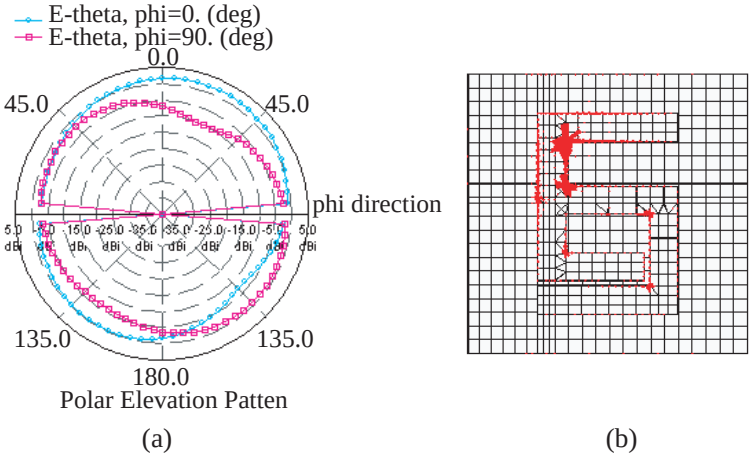

Figure 12. Radiation pattern and current distribution at the second resonance (1500 MHz band). (a) Radiation pattern, (b) Current distribution.

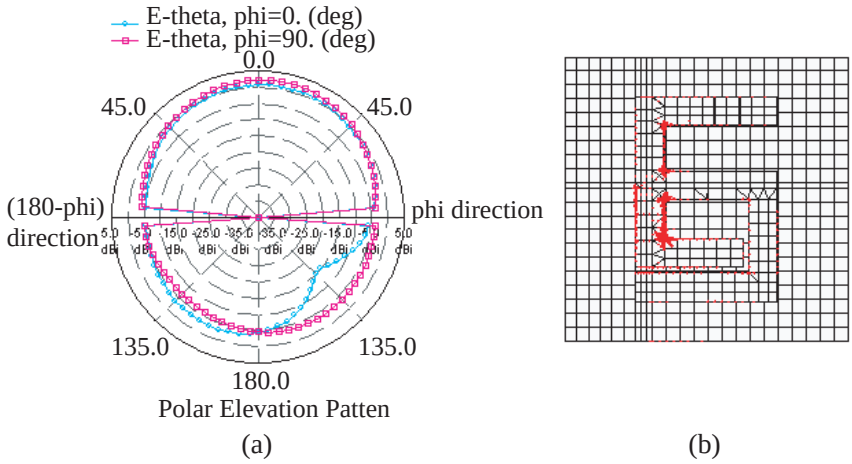

Figure 13. Radiation pattern and current distribution at the third resonance (1800 MHz band). (a) Radiation pattern, (b) Current distribution.

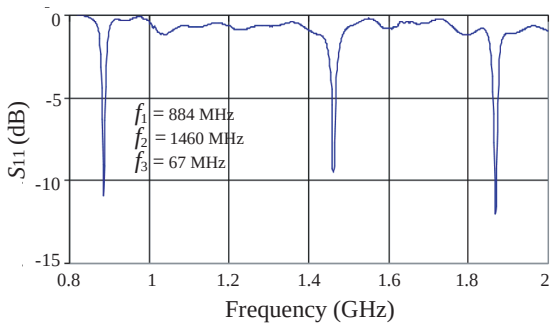

Figure 14. Measured S_{11} of the proposed modified E-shaped triple band antenna.

RT/Duroid substrate used in the theoretical study. The measurements have been performed using Vector network Analyzer. The measured results are shown in Fig. 14. Good agreement between the simulated and the measured results is observed. The measured resonance frequencies are 884 MHz, 1460 MHz, and 1867 MHz. The first and third resonance frequencies are very close to that obtained by the simulated results. However, a 46 MHz frequency shift is noticed at the second frequency. This shift can be easily adjusted by slightly decreasing the length of branch 3. The matching performance is quite good

but less than the simulated values, especially at the second resonance, 1460 MHz. This is attributed to the limited accuracy of the available feed mounting tools.

7. CONCLUSION

Two new triple band compact microstrip antenna structures for wireless communications have been investigated. The proposed antenna configurations, each is the integration of three resonant elements designed separately at three pre-specified bands. The outlined design approach is simple and can be applied to design any triple band antenna at three pre-specified bands on any suitable substrate. The resonator integration has been performed to reduce the overall antenna size and maintain the performance of each element. The composed three resonators share single common feed and short-circuit probe. Basic triple-band antenna designs are performed using simple curves and formulas for compact short-circuited stepped impedance and quarter-wave resonators. The designed antennas are simulated using a full wave EM simulator and then realized on RT/Duroid dielectric substrate material with 2.2 relative permittivity and 1.57 mm thickness. The design concept and the performance of the presented composite compact triple-band antennas are verified by simulation and measurements.

REFERENCES

1. Rowell, C. R. and R. D. Murch, "A compact PIFA suitable for dual-frequency 900/1800-MHz operation," *IEEE Trans. Antennas Propagat.*, Vol. 46, 596–598, April 1998.
2. Sim, C. Y. D., "A novel dual frequency PIFA design for ease of manufacturing," *Journal of Electromagnetic Waves and Applications*, Vol. 21, No. 3, 409–419, 2007.
3. Elsadek, H. and D. Nashaat, "Ultra miniaturized E-shaped dual band PIFA on cheap foam and FR4 substrates," *Journal of Electromagnetic Waves and Applications*, Vol. 20, No. 3, 291–300, 2006.
4. Wu, G.-L., W. Mu, G. Zhao, and Y.-C. Jiao, "A novel design of dual circularly polarized antenna feed by L-strip," *Progress In Electromagnetics Research*, PIER 79, 39–46, 2008.
5. Geyi, W., Q. Rao, S. Ali, and D. Wang, "Handset antenna design: practice and theory," *Progress In Electromagnetics Research*, PIER 80, 123–160, 2008.

6. Ren, W., "Compact dual-band slot antenna for 2.4/5 GHz WLAN applications," *Progress In Electromagnetics Research B*, Vol. 8, 319–327, 2008.
7. Naghshvarian-Jahromi, M., "Novel miniature semi-circular-semi-fractal monopole dual band antenna," *Journal of Electromagnetic Waves and Applications*, Vol. 22, No. 2–3, 227–237, 2008.
8. Wang, C.-J. and S.-W. Chang, "Studies on dual-band multi-slot antennas," *Progress In Electromagnetics Research*, PIER 83, 293–306, 2008.
9. Alkanhal, M. and A. F. Sheta, "A novel dual-band reconfigurable square-ring microstrip antenna," *Progress In Electromagnetics Research*, PIER 70, 337–349, 2007.
10. Song, Y., Y.-C. Jiao, G. Zhao, and F.-S. Zhang, "Multiband CPW-FED triangle-shaped monopole antenna for wireless applications," *Progress In Electromagnetics Research*, PIER 70, 329–336, 2007.
11. Zhao, G., F.-S. Zhang, Y. Song, Z.-B. Weng, and Y.-C. Jiao, "Compact ring monopole antenna with double meander lines for 2.4/5 GHz dual-band operation," *Progress In Electromagnetics Research*, PIER 72, 187–194, 2007.
12. Song C. T. P., P. S. Hall, H. Ghafouri-Shiraz, and D. Wake, "Triple band planar inverted F antennas for handheld devices," *Electron. Lett.*, Vol. 36, No. 2, 112–114, 2000.
13. Hsiao, F. R. and K. L. Wong, "Compact planar inverted-F patch antenna for triple-frequency operation," *Microwave Opt. Technol. Lett.*, Vol. 33, 459–462, June 2002.
14. Dou, W. P. and Y. W. M. Chia, "Novel meandered planar inverted-F antenna for triple-frequency operation," *Microwave Opt. Technol. Lett.*, Vol. 27, 58–60, Oct. 5, 2000; *Dig.,* 112–115.
15. Ansari, J. A., P. Singh, S. K. Dubey, R. U. Khan, and B. R. Vishvakarma, "H-shaped stacked patch antenna for dual band operation," *Progress In Electromagnetics Research B*, Vol. 5, 291–302, 2008.
16. Kuo, L.-C., "Analysis of a 900/1800-MHz dual-band gap loop antenna on a handset with proximate head and hand model," *Journal of Electromagnetic Waves and Applications*, Vol. 21, No. 1, 107–122, 2007.
17. Wu, Y.-J., B.-H. Sun, J.-F. Li, and Q.-Z. Liu, "Triple-band omni-directional antenna for WLAN applications," *Progress In Electromagnetics Research*, PIER 76, 477–484, 2007.
18. Singh, D., C. Kalialakis, P. Gardner, and P. S. Hall, "Small H-

shaped antennas for MMIC applications," *IEEE Trans. Antennas Propagat.*, Vol. 48, 1134–1140, July 2000.

19. Mohra, A., A. F. Sheta, and S. F. Mahmoud, "Analysis and design of small size short circuited microstrip T-shaped antenna," *Proc. of 20th National Radio Science Conference*, B18, Cairo, Egypt, 2003.
20. Sheta, A. F. and M. Alkanhal, "Compact dual-band tunable microstrip antenna for GSM/DCS-1800 applications," *IET Microwave Antenna and Propagation*, Vol. 2, No. 3, 274–280, 2008.
21. Wong, K.-L. and Y. F. Lin, "Small broad band rectangular MSA with chip resistor loading," *Electron. Lett.*, Vol. 33, No. 19, 1593–1594, 1997.
22. Lu, J. H. and K. P. Yang, "Slot coupled compact triangular microstrip antenna with lumped load," *Proc. IEEE AP-Symp.*, 916–919, 1998.
23. Albooyeh, M., N. Kamjani, and M. Shobeyri, "A novel cross-slot geometry to improve impedance bandwidth of microstrip antennas," *Progress In Electromagnetics Research Letters*, Vol. 4, 63–72, 2008.